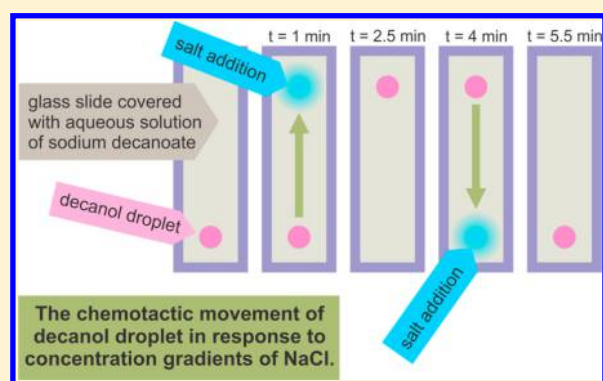


## Dynamics of Chemotactic Droplets in Salt Concentration Gradients

Jitka Čejková,<sup>\*,†,‡</sup> Matěj Novák,<sup>†</sup> František Štěpánek,<sup>†</sup> and Martin M. Hanczyc<sup>‡,§</sup><sup>†</sup>Chemical Robotics Laboratory, Institute of Chemical Technology Prague, Technická 3, 166 28 Prague 6, Czech Republic<sup>‡</sup>Center for Fundamental Living Technology (FLIN<sup>T</sup>), Department of Physics, Chemistry and Pharmacy, University of Southern Denmark, Campusvej 55, DK-5230 Odense M, Denmark<sup>§</sup>Centre for Integrative Biology CIBIO, University of Trento, via delle Regole 101, 38123 Mattarello (TN), Italy

## Supporting Information

**ABSTRACT:** The chemotactic movement of decanol droplets in aqueous solutions of sodium decanoate in response to concentration gradients of NaCl has been investigated. Key parameters of the chemotactic response, namely the induction time and the migration velocity, have been evaluated as a function of the sodium decanoate concentration and the NaCl concentration gradient. The ability of the decanol droplets to migrate in concentration gradients has been demonstrated not only in a linear chemotactic assay but also in a topologically complex environment. Additionally, the ability to reverse the direction of movement repeatedly, to carry and release a chemically reactive cargo, to select a stronger concentration gradient from two options, and to initiate chemotaxis by an external temperature stimulus have been demonstrated.



## 1. INTRODUCTION

The locomotion of live cells is a highly complex process involving various biochemical and biophysical elements.<sup>1</sup> Motion is usually associated with motor proteins that convert chemical energy to mechanical work. The movement of freely living cells can be caused by special organelles for locomotion such as cilia and flagella or by migration over solid substrates by crawling or gliding, i.e., by coordinated changes in shape and adhesivity to a substrate in response to environmental stimuli, using pseudopodia. The latter mechanism is manifested by single-cell organisms such as amoebae, diatoms, and some types of cyanobacteria and human leukocytes.

The swimming and crawling movements of cells can be random or oriented. Cells usually move because this takes them closer to a source of nutrients or further away from a source of harmful compounds. Such extracellular chemical cues (nutrients, pheromones, repellents, toxins) guide the movement of a cell in a particular direction—a process called chemotaxis.<sup>2</sup> Chemotaxis can be positive (movement toward a chemo-attractant) or negative (movement away from a repellent). Chemotaxis differs from chemokinesis, in which case the signal substance merely alters the rate or frequency of random motion.<sup>3</sup>

The movement of nonliving objects in concentration gradients (artificial chemotaxis) can be based on several different mechanisms. The movement of asymmetric bimetallic catalytic rods or spheres in the concentration gradient of H<sub>2</sub>O<sub>2</sub> has been reported.<sup>4</sup> In this case, a catalytic chemical reaction produces gas bubbles that propel the particles. Similarly, Mano and Heller<sup>5</sup> described a system based on a carbon fiber having a

terminal glucose oxidizing microanode and an O<sub>2</sub> reducing microcathode, which was propelled at the H<sub>2</sub>O–O<sub>2</sub> interface. It was shown that the diffusiophoretic phenomenon shares similarities with chemotaxis.<sup>6</sup> When a rigid colloidal particle is placed in a solution with nonuniform concentration of a solute that interacts with the particle, the particle can move along the concentration gradient of the solute. It has also been shown that dynamic cytoskeletal components, biomolecular motors (kinesin, myosin), and their associated filaments (microtubule, actin) can be combined *in vitro* with synthetic components to create nanoscale transport systems.<sup>7</sup> Synthetic phospholipid vesicles coated by proteins that initiate actin polymerization displayed the ability to propel lipid vesicles in a similar way as in *Listeria* cells.<sup>8</sup> Hybrid objects containing an artificial component and living organism have also been suggested.<sup>9</sup>

An alternative mechanism of artificial chemotaxis is based on “self-running” objects at interfaces. Alcohol droplets<sup>10</sup> or pieces of camphor<sup>11</sup> on a water surface can move due to a surface tension gradient caused by the gradual dissolution of the object itself. An oil droplet can also move on a solid substrate when the surface underneath the droplet is asymmetrically modified and causes a difference in the interfacial energy between the leading and the trailing edge of the droplet.<sup>12</sup> Grzybowski and co-workers showed a droplet of mineral oil and 2-hexyldecanoic acid in a labyrinth with a pH gradient, where the droplets were able to find the shortest path through the maze.<sup>13</sup>

Received: July 3, 2014

Revised: August 4, 2014

The self-propelled motion of a droplet can be coupled with a chemical reaction that occurs at the interface between the droplet and the surrounding medium. The chemical reaction can result in a symmetry breakage due to the accumulation and release of the reaction products, and the droplets can move through the aqueous medium without the need of an air–water or a solid–liquid interface. A system of oil droplet movement based on fatty acid chemistry has been proposed by Hanczyc et al.<sup>14</sup> An oil phase containing oleic anhydride precursor was introduced into an aqueous environment that contained oleate micelles. The products of the precursor hydrolysis were coupled to the movement of the oil droplet and the production of waste vesicles. The oil droplet successfully moved away from this waste product into fresh unmodified solution, displaying a form of chemotaxis. This example mimics the behavior of cells that move away from their metabolic products into regions with fresh nutrients. Similar experiments with different chemicals were performed in ref 15.

In the present work, a new artificial chemotaxis system is introduced, based on decanol droplets moving in aqueous solution of sodium decanoate along concentration gradients of sodium chloride. The parametric dependence of the chemotactic response with respect to background concentration of sodium decanoate and the strength of the NaCl concentration gradient has been investigated. Several scenarios that utilize chemotaxis—namely, migration over a nonlinear path, delivery of a chemically reactive cargo, selection of the direction of motion according to the strength of the chemoattractant source, and temperature-triggered release of the chemoattractant—have been demonstrated.

## 2. EXPERIMENTAL SECTION

**2.1. Materials and Methods.**  $\beta$ -Carotene, decanoic acid, decanol, iodine, nitrobenzene, oil red O, paraffin, sodium chloride, and sodium hydroxide were obtained from Sigma-Aldrich. Decanoic acid solutions in the aqueous phase were prepared at the desired concentration (typically 10 mM) in water using 5 M NaOH to raise the pH of the resulting solution, typically to 10–13. Menzel-Gläser microscope slides 76 × 26 mm and 75 × 50 mm (Thermo Scientific) and an adhesive double sided tape (3M 468MP 200MP) were used for the preparation of chemotactic assays.

**2.2. Chemotactic Assays.** The edges of a microscopic slide were covered with thin strips of adhesive tape to form a shallow pool with a rectangular shape. The pool was filled by 1 mL of decanoate (5 or 10 mM) or water, and then a 5  $\mu$ L decanol droplet containing oil red O as a colorant was placed at one side of the slide. After approximately 1 min, droplets of NaCl were added to the opposite side. The droplet volume was chosen so as not to alter the liquid level in the pool to an extent that would cause bulk fluid flow or movement of the decanol droplet. (This was verified by adding water droplets without NaCl under otherwise identical experimental conditions and noting that this did not induce any movement of the decanol droplet.) The distance between the decanol and the NaCl droplets was systematically varied to create different concentration gradients. The molar quantity of added NaCl was also systematically varied in the range 5–100  $\mu$ mol by changing the salt concentration. The movement of the decanol droplet toward higher NaCl concentration was monitored using a PixelINK camera (PL-A662) and later processed by NIS-Elements software (Laboratory Imaging Ltd., Czech Republic). From the droplet trajectory ( $X$  and  $Y$  coordinates as a function of time), the induction time and the migration velocity were evaluated.

For temperature-triggered chemotaxis experiments, the NaCl concentration gradient was not formed by adding saline droplets but by liberating small NaCl crystals from a paraffin matrix by the local application of a heat source that melted the paraffin. Fine NaCl grains were first dispersed in molten paraffin, from which small spheres were

manually formed upon cooling. The salt-loaded paraffin spheres were then repeatedly washed by deionized water to remove any salt grains that may be at the surface. A single NaCl-loaded paraffin sphere was then carefully placed to one side of the chemotactic assay where it acted as a temperature-responsive salt reservoir.

**2.3. Surface Tension Measurements.** Surface tension measurements of decanoate solutions with varying concentrations of NaCl and decanol were performed using the Wilhelmy plate method (tensiometer Sigma 703 D, Attension). The purpose of the surface tension measurements was to verify a hypothesis about Marangoni flow as a possible cause of the observed chemotaxis (translation of concentration gradients to gradients of surface tension).

## 3. RESULTS AND DISCUSSION

### 3.1. Chemotaxis of Decanol Droplets in Rectangular Cells. Figure 1 shows the trajectory of a 5 $\mu$ L decanol droplet

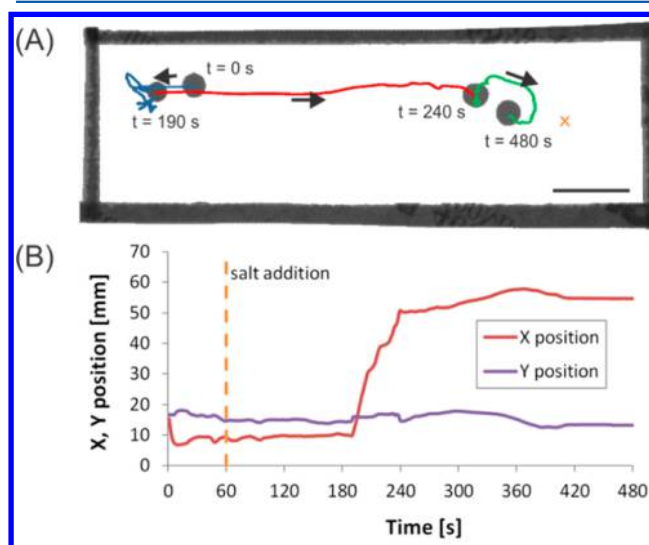


**Figure 1.** (A) Trajectory of a 5  $\mu$ L decanol droplet in a rectangular pool (76 × 26 mm) containing 1 mL of 10 mM sodium decanoate. The orange cross indicates the place of salt addition, which occurred at  $t = 60$  s. Scale bar represents 1 cm. (B) The  $X$  and  $Y$  positions of the droplet as a function of time, evaluated from the trajectory. The orange line indicates the moment of salt addition at  $t = 60$  s.

in 1 mL of a 10 mM decanoate solution contained in a rectangular pool with the size 76 × 26 mm (cf. section 2.2). The droplet started on the left-hand side of the rectangular pool, and its movement was initially random. After 1 min, a 10  $\mu$ L droplet of a 5 M NaCl solution (i.e., 50  $\mu$ mol of NaCl) was added to the right-hand side of the microscopic slide. The decanol droplet continued its random movement on the left side of the slide (blue trajectory in Figure 1A), but after a certain induction time it started to follow the salt concentration gradient and performed an almost straight oriented movement to the opposite end of the pool (red trajectory in Figure 1A). Once the decanol droplet reached the area where the salt droplet was added, it has returned to a random, local movement (green trajectory in Figure 1A). A video recording of the entire experiment can be found in Supporting Information Movie 1.

The graph in Figure 1B shows the  $X$  and  $Y$  coordinates of the decanol droplet as a function of time, evaluated from the droplet trajectory (Figure 1A). Without a salt concentration gradient, the droplet moves locally and randomly, with no apparent directionality. It is interesting to note from Figure 1B that the droplet does not respond by chemotaxis immediately

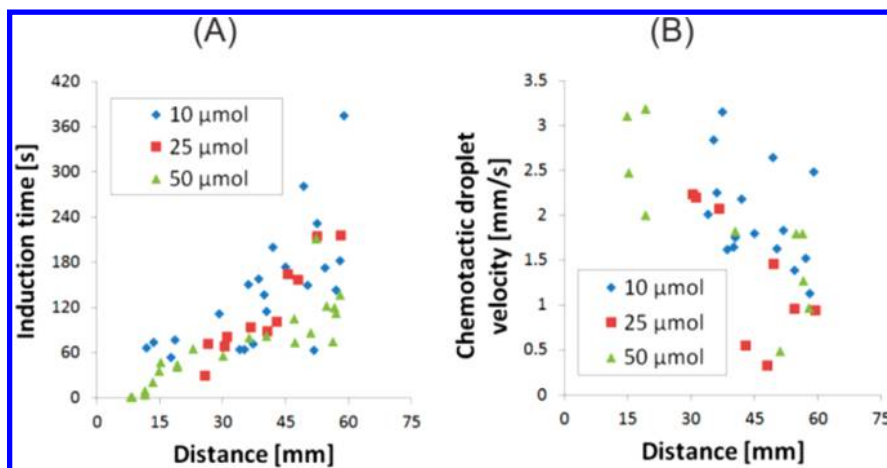


**Figure 2.** (A) Dependence of the chemotaxis induction time on the initial distance between the decanol and salt droplets for various molar quantities of added NaCl. (B) Dependence of the decanol droplet velocity during chemotaxis on the same parameters as in case (A).

after the salt addition (indicated by a vertical line at  $t = 60$  s). Presumably this lag period corresponds to the time that is necessary for a concentration or interfacial tension gradient caused by NaCl addition to reach the decanol droplet. Once the signal reaches the decanol droplet, the droplet migrates toward the source of the gradient (the point of salt droplet deposition) at an increased speed as indicated by the slope of the  $X$  vs time trajectory in Figure 1B.

It can be expected that the induction time, i.e., the delay between NaCl addition and the start of chemotaxis of the decanol droplet, should be related to the time of the “chemical signal” propagation from the NaCl droplet to the decanol droplet. The underlying transport mechanism includes not only the diffusion of NaCl (see Supporting Information) but also convection. In the case of convection the flow can be due to a density difference or due to an interfacial tension gradient. The dependence of the induction time on the molar quantity of added NaCl and on the initial distance between the decanol droplet and the point of salt addition is summarized in Figure 2A (the volume of the added NaCl droplet was kept constant as well as all other parameters of the experiment). Despite the relatively widespread observed induction times, two trends are evident: the induction time increases with increasing distance, and the induction time decreases with increasing salt concentration.

It should be noted that there exists a finite window of NaCl concentrations at which chemotaxis has occurred. Both lower ( $5 \mu\text{mol}$ ) and higher ( $100 \mu\text{mol}$ ) salt additions were also tested, but neither has led to chemotaxis. The  $5 \mu\text{mol}$  addition was insufficient to induce a chemotactic response whereas in the case of  $100 \mu\text{mol}$  the decanol droplet responded by a brief jerky movement toward the salt addition point, but only over a short distance. The decanol droplet did not move across the entire slide as in the case of salt additions in the range  $10$ – $50 \mu\text{mol}$ . This behavior bears interesting similarity with one of the best-studied examples of biological chemotaxis, i.e., the migration of *Dictyostelium* amoebae in concentration gradients of cyclic adenosine-3',5'-monophosphate (cAMP).<sup>16,17</sup> In the absence of cAMP, the cells are not at rest but perform a random motion with an average motility of  $4.2 \mu\text{m}/\text{min}$ .<sup>18</sup> At intermediate cAMP gradients, the cells move up the gradient with an average motility of  $9 \mu\text{m}/\text{min}$ . In very steep gradients (above  $10 \text{ nM}/\mu\text{m}$ ) the cells again lose directionality and revert to random motion.

The velocity of droplet movement was also evaluated as the slope of the  $X$  position vs time (as in Figure 1B) for all distance–concentration combinations, and the results are summarized in Figure 2B. In this case, the chemotactic velocity of the decanol droplet is a decreasing function of the initial distance, but there does not seem to be any systematic dependence on the molar quantity of added NaCl.

The migration speed during chemotaxis is usually considered to be proportional to the concentration gradient of the chemoattractant. However, the results observed here do not fully agree with this assumption. If the gradient is defined as the concentration difference divided by distance, then a 5-fold increase in the quantity of added NaCl (e.g., from  $10$  to  $50 \mu\text{mol}$ ) should have the same effect as a 5-fold decrease in distance (e.g., from  $50$  to  $10 \text{ mm}$ ). It is evident from Figure 2B that while a change in the droplet distance clearly leads to a proportional change in the chemotactic migration velocity, a corresponding change in the salt concentration does not. This may be due to the salting out of the decanoate surfactant in areas of very high NaCl concentrations. This is sometimes confirmed visually by the appearance of a white turbid substance at the position of highest salt concentration.

**3.2. Reversal of Chemotaxis Direction.** The ability of the decanol droplet to respond by chemotaxis to repeatedly created salt concentration gradients was investigated (Figure 3, Supporting Information Movie 2). The experimental setup was similar as that discussed in section 3.1, i.e., a  $5 \mu\text{L}$  decanol

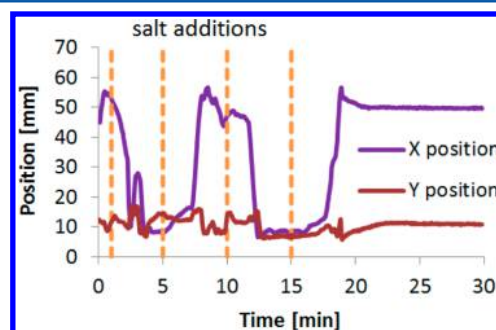


**Figure 3.** X and Y positions of a  $5 \mu\text{L}$  decanol droplet in a rectangular pool containing  $5 \text{ mM}$  sodium decanoate solution, subjected to repeated salt additions (each containing  $50 \mu\text{mol}$  of NaCl) at times  $t = 1, 5, 10,$  and  $15$  min.

droplet in a rectangular pool of a sodium decanoate solution. However, instead of a single salt droplet addition, a droplet containing 50  $\mu\text{mol}$  of sodium chloride was added four times at 5 min intervals (specifically, at time  $t = 1, 5, 10,$  and  $15$  min) alternatively to opposite ends of the pool. The interval of 5 min was sufficiently long to include the induction time, chemotactic migration of the decanol droplet toward the salt addition point, and stabilization of the droplet at the final location. The  $X$  and  $Y$  coordinates of the decanol droplet resulting from the repeated salt additions are shown in Figure 3. Note that although the total molar quantity of the added salt has gradually accumulated to 200  $\mu\text{mol}$ , chemotaxis still took place after the fourth salt addition. Therefore, increased background salt concentration does not appear to be a hindrance to chemotaxis, as long as a concentration gradient is re-established.

**3.3. Ink Tracer Experiments.** The experiments described above imply that the existence of a salt concentration gradient triggers the chemotactic movement of the decanol droplet, but the underlying interactions can be complex. A key question is whether the observed decanol droplet movement is caused by Marangoni flow due to a surface tension gradient or if there are also other types of flow involved, e.g., due to density difference or contact angle gradient.

The progress of two experiments where an ink tracer was used to visualize the flow pattern in the surrounding aqueous fluid is shown in Figure 4 and in Supporting Information Movie 3. A rectangular pool with 1 mL of a 10 mM decanoate solution

was used, and the order in which the decanol and the NaCl solution droplets were added was changed. The initial ink patterns were created by dropping a small amount of ink solution onto the surface of the decanoate pool and then gently mixing the surface layer by a pipet tip (see Supporting Information Movie 3). Neither convective flows nor surface tension changes were observed. Once the decanol droplet was added (time  $t = 40$  s in Figure 4A), the original ink patterns immediately disappeared due to a reduction of surface tension near the decanol droplet and Marangoni flow toward regions of high surface tension, i.e., away from the decanol droplet. Decanol acts as a surfactant, and its effects on the surface tension of 10 mM decanoate solution, measured separately (cf. section 2.3), are summarized in Figure 5A. The addition of a salt droplet colored by blue food dye (time  $t = 60$  s in Figure 4A) did not cause any visible changes in the ink pattern. The salt solution did not attract or repel the ink particles (no diffusiophoresis was observed). However, the salt droplet did not spread uniformly and had a tendency to spread somewhat faster toward the decanol droplet (tear-like blue spot at  $t = 80$  s in Figure 4A). The decanol droplet eventually moved chemotactically to the area of the salt addition (time  $t = 120$  s in Figure 4A).

When the order of the droplet addition was reversed, i.e., adding the salt droplet first and the decanol droplet next (in Figure 4B), no change in the initial ink pattern was observed after salt addition despite the fact that NaCl also slightly reduces the surface tension of decanoate solution (Figure 5B). The salt spot spread uniformly in all directions and did not affect the ink pattern ( $t = 40$  s in Figure 4B). The decanol droplet addition rapidly deleted the ink patterns and repelled the ink to the opposite end of the glass slide ( $t = 60$  s in Figure 4B). The salt started to flow toward decanol ( $t = 80$  s in Figure 4B), and the decanol droplet was transported chemotactically to the zone of the salt droplet addition ( $t = 120$  s in Figure 4B).

Several additional experiments with an ink tracer in a single chamber with and without obstacles were done, and the results are shown in Supporting Information Movie 3. The black ink served as tracer to visualize the convective flow in the aqueous phase. Both direct salt solution addition and salt diffusion from nitrobenzene droplets were tested. The blue spot of salt had a tendency to spread toward the decanol droplet due to directional flow of the aqueous phase. In all cases the shortest path between the decanol droplet and the salt source was highlighted, and the decanol droplet followed this path and moved chemotactically toward the salt. In experiments with nitrobenzene droplets loaded with salt grains, fusion with the decanol droplet occurred.

**3.4. Nonlinear Path Experiments.** In the experiments described above, it was shown that decanol droplets follow a salt concentration gradient created by direct addition of a salt solution. In order to sustain a concentration gradient for longer periods of time without disturbing the system by repeated external liquid additions, an alternative method of creating the salt concentration gradient has been used—a nitrobenzene droplet loaded with NaCl grains was deposited in the decanoate pool instead of an aqueous droplet with predissolved NaCl (Supporting Information Movie 4). The nitrobenzene droplet (which is immiscible with water) was stationary and allowed a gradual leaching of NaCl to the surrounding solution. This created a salt concentration gradient, which in turn resulted in a chemotactic movement of the decanol droplet toward the nitrobenzene droplet, eventually fusing with it. Independent

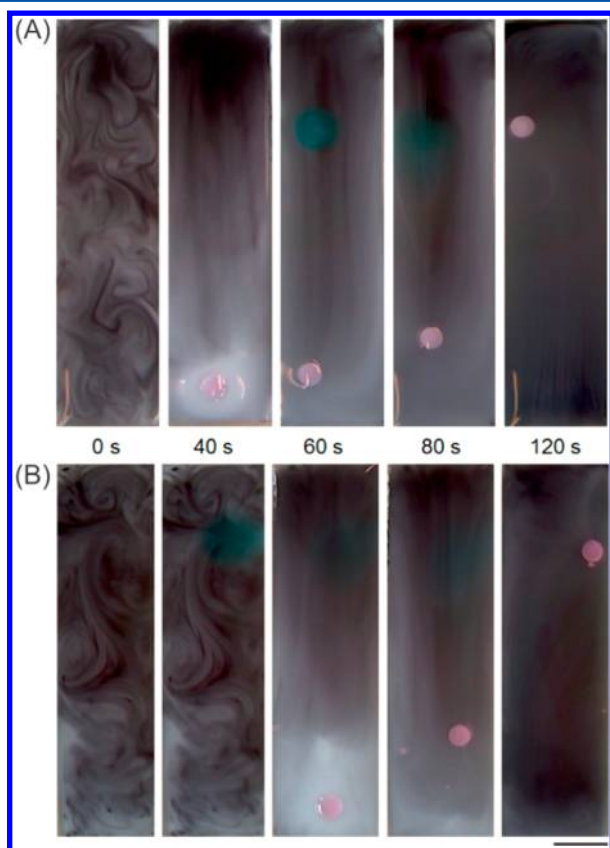


**Figure 4.** Flow field visualization using ink tracer: (A) decanol droplet addition followed by salt addition; (B) salt droplet addition followed by decanol addition. The decanol droplet was deposited at the bottom end of the rectangular pool and was labeled by a pink color; the salt droplet (deposited at the top end) is blue. Scale bar represents 1 cm.

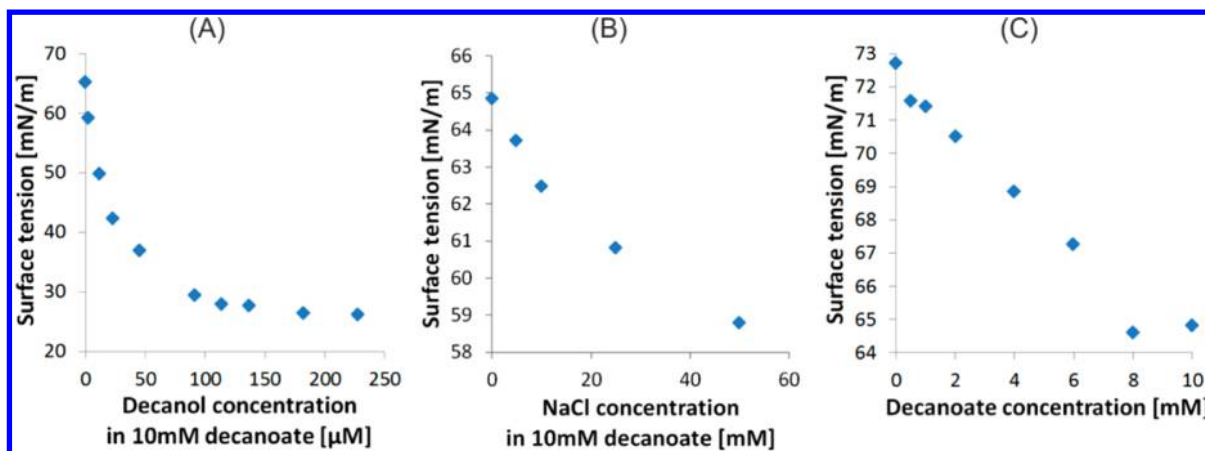


**Figure 5.** Dependence of the surface tension of 10 mM decanoate solution on (A) decanol and (B) NaCl concentration. (C) Dependence of the surface tension of water on the sodium decanoate concentration.

verification experiments have shown that without NaCl there is no interaction between the nitrobenzene and decanol droplets, i.e., no chemotaxis and no fusion.

The salt concentration gradients created by the nitrobenzene droplet with salt grains were used in scenarios where the chemotaxis of the decanol droplet took place over a nonlinear path in slightly more complex topologies than a straight channel. Two examples of such topologies are shown in Figure 6. In each case, the decanol droplet followed the shortest path toward the source of the salt and eventually fused with the salt-loaded nitrobenzene droplet.

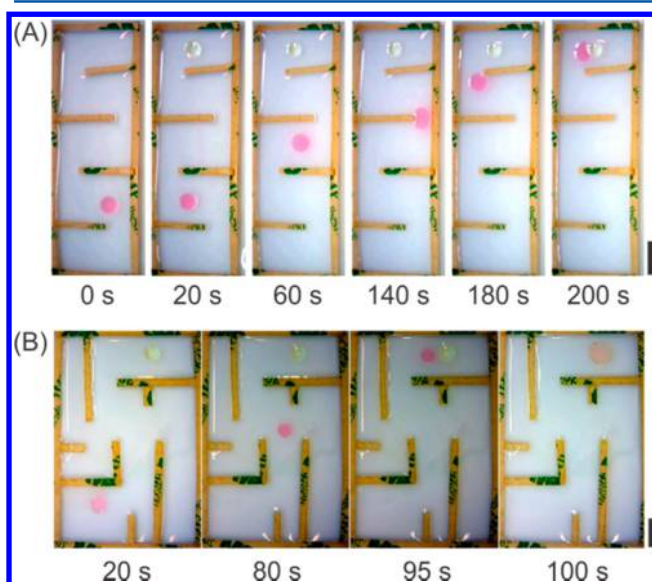


**Figure 6.** Examples of droplet chemotaxis in a complex topology: (A) nonlinear path in a channel; (B) nonlinear path in a simple "labyrinth" with dead end channels. The decanol droplet has a purple color, and the salt diffuses from a stationary nitrobenzene droplet (yellowish color). Scale bar represents 1 cm.

Although the topology shown in Figure 6B could theoretically allow the decanol droplet to follow an incorrect path into a dead-end channel, there was only one source of the salt gradient. An alternative scenario was therefore realized, where the decanol droplet had two alternatives, i.e., two sources of salt located at an identical distance but in opposite ends of the pool (see Figure 7). The two sources contained a different

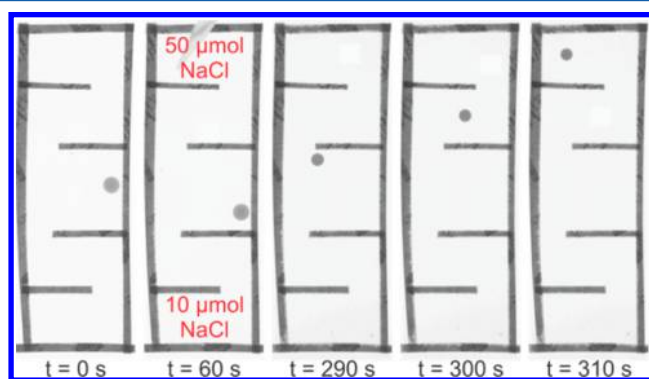


**Figure 7.** Decanol droplet (middle of the pool at  $t = 0$  s) attracted by a stronger salt concentration gradient. Scale bar represents 1 cm.

quantity of NaCl, namely 50 and 10  $\mu\text{mol}$ . The decanol droplet, initially located in the middle of the pool, started to migrate toward the end with a higher concentration of salt. Thus, two important features of chemotaxis, also revealed by living systems, were demonstrated: the ability to follow the chemoattractant in a complex topology and the ability to follow a stronger source of chemoattractant when presented with alternative chemotaxis directions.

**3.5. Stimulus-Responsive Release of Chemoattractant.** The diffusion of NaCl from the nitrobenzene droplet, discussed in the previous section, was spontaneous. However, in nature, the release of a chemoattractant is often triggered by a change in some environmental variable, for example temperature, which can signal conditions favorable for the next phase of a reproduction cycle. A similar scenario of temperature-triggered release of the chemoattractant has been realized in laboratory conditions as follows. Instead of a nitrobenzene droplet, fine NaCl crystals were encapsulated into a paraffin particle with a melting point of 42  $^{\circ}\text{C}$  as described in section 2.2.

When a single salt-containing wax sphere was deposited into a pool of sodium decanoate at low temperature, the salt could not diffuse from the paraffin particle in the solid state and the system was stationary. However, once the paraffin particle was locally heated to a temperature above its melting point, the previously encapsulated salt was liberated, started to dissolve in the surrounding solution, and triggered the chemotaxis of the decanol droplet, which migrated toward to source of salt

(Figure 8, Supporting Information Movie 5). As in the case of nitrobenzene, a control experiment without NaCl (only paraffin and heating) did not lead to chemotaxis or thermophoresis.

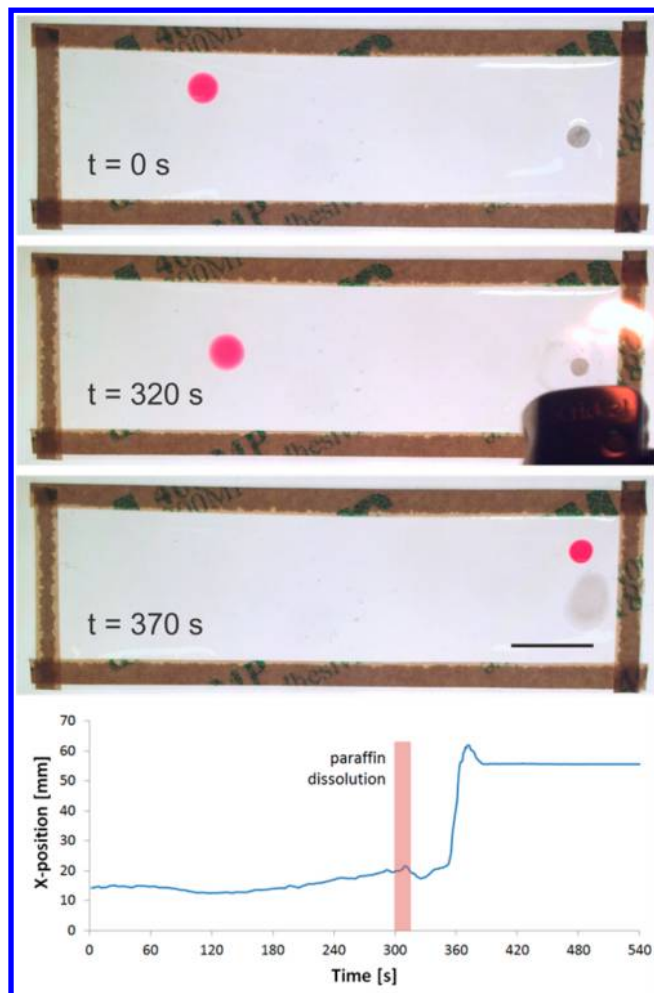


**Figure 8.** (A) Progress of an experiment with a paraffin particle containing salt grains as a thermoresponsive source of chemoattractant. The chemotactic decanol droplet is marked by a pink color; the paraffin particle is gray. Scale bar represents 1 cm. (B) Trajectory of the decanol droplet, evaluated from the experiment. Local heating of the paraffin particle was applied at  $t = 300$  s for 20 s and resulted in NaCl liberation from the particle.

**3.6. Chemotaxis Delivery of a Reactive Payload.** It has been shown in the previous sections that a decanol droplet is able to locate a nitrobenzene droplet and fuse with it even in topologically complex environments and that it is able to follow the strongest source of chemoattractant from several alternatives. These are the prerequisites for the laboratory demonstration of a model “search-and-neutralize” mission, whereby the chemotactic droplet carries a payload that will react with the chemoattractant source once the mobile droplet localizes it. Again, an analogy with natural systems can be seen in this scenario, e.g., the chemotaxis of a leukocyte that actively locates and eventually neutralizes a pathogen.

Decanol was saturated with solid iodine to produce a dark orange oil. Independently,  $\beta$ -carotene was added to pure nitrobenzene and mixed to obtain a red oil at 2 mg/mL. Droplets of 10  $\mu$ L of each solution were added to opposite ends of a channel with a simple obstacle in the middle, filled with 10

mM decanoate (pH 11). The progress of the experiment is shown in Figure 9. After chemotaxis and fusion of the decanol and nitrobenzene droplets, a color change to green indicated that an iodination reaction of  $\beta$ -carotene has taken place.<sup>19</sup>

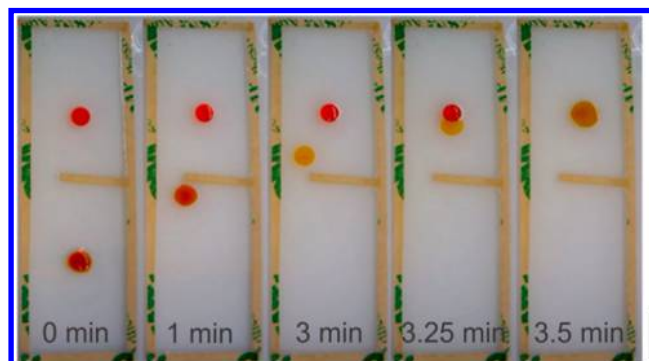


**Figure 9.** Example of a chemotactic droplet carrying a reactive payload toward the chemoattractant source (iodination assay). The chemotactic decanol droplet moves from the bottom to the top section of the figure and eventually fuses with the stationary nitrobenzene droplet. The chemical reaction is indicated by a color change. Scale bar represents 1 cm.

**3.7. Chemotaxis Mechanism and Force Balance.** The decanol droplet in a homogeneous solution of decanoate exhibits weak random motion, as shown in Figure 1. This is likely due to the loss of mass of the droplet over time because the droplet itself is slowly being dissolved into the surrounding soapy solution. However, when a salt gradient is introduced to the system, a corresponding surface tension gradient is established (Figure 5). There are several works where it was shown experimentally and theoretically how surface tension gradients give rise to convective flows that result in particle or droplet motion.<sup>20,21</sup> There are two possible theoretical approaches—a fluid mechanics approach based on the solution of the Navier–Stokes equations or a simplified force balance approach whereby the moving object is regarded as a rigid body subjected to Newton’s law of motion. The latter approach, adopted from ref 21, is adopted here.

Let us assume that the decanol droplet has a constant mass. The net force acting on the decanol droplet due to a gradient of surface tension and due to fluid–fluid and wall–fluid friction is

$$m \frac{dv_{\text{drop}}}{dt} = F_A - F_D - F_W \quad (1)$$

where  $m$  is the droplet mass,  $v_{\text{drop}}$  is the macroscopic droplet velocity,  $F_A$  is the surface tension force,  $F_D$  is the fluid–fluid drag force, and  $F_W$  is the fluid–wall drag force. If the surface tension force is greater than the frictional and drag forces, locomotion of the droplet can occur.<sup>22,23</sup> Let us now estimate the magnitude of the forces for our system.

In the case of a shallow pool, the total concentration of NaCl in the solution of sodium decanoate is known (50 mM). Since the dependence of surface tension on NaCl concentration was independently measured (Figure 5), the salt concentration gradient can be translated into a gradient of surface tension. Assuming a linear concentration gradient and a pool length of 70 mm, the corresponding macroscopic surface tension gradient is  $\partial\gamma/\partial x = 173.5$  mN/m<sup>2</sup>. The diameter of the droplet projection in this setup, obtained through image analysis, is 3.6 mm. By using these values, an order-of-magnitude estimate of

the force acting on the droplet due to the surface tension gradient can be made. Using the divergence theorem, the integration along the circumference of the droplet can be replaced by

$$F_A = \oint_{\partial A} \mathbf{i} \cdot \mathbf{n} \gamma dl = \int_A (\nabla \cdot \mathbf{i} \gamma) dA = \int_A \left( \frac{\partial \gamma}{\partial x} \right) dA = \left( \frac{\partial \gamma}{\partial x} \right) A \quad (2)$$

where  $A = 10.18 \times 10^{-6} \text{ m}^2$  is the projected droplet area and  $\mathbf{i} = [1, 0, 0]$  is a unit vector in the direction of the macroscopic surface tension gradient. The resulting force is  $F_A = 1.77 \times 10^{-6} \text{ N}$ . The force due to a surface tension gradient would be opposed by viscous dissipation in the fluid.

As an order-of-magnitude estimate of these effects, let us consider the droplet to be a rigid sphere and evaluate the Stokes drag force according to

$$F_D = 6\pi\eta r v_{\text{drop}} \quad (3)$$

where  $\eta = 10^{-3} \text{ Pa}\cdot\text{s}$  is viscosity (assuming equal to that of water for the purpose of the estimate),  $v_{\text{drop}} = 1.5 \times 10^{-3} \text{ m/s}$  is a characteristic value of the droplet velocity (cf. Figure 2B), and  $r = 1.06 \times 10^{-3} \text{ m}$  is the characteristic droplet radius computed directly from its volume. The resulting drag force is  $F_D = 0.03 \times 10^{-6} \text{ N}$ , which is significantly lower than the force due to surface tension gradient, although it is in fact an overestimate because the decanol droplet is not fully surrounded by the aqueous phase. Similarly, an estimate of the upper value of the wall friction force can be made by assuming the decanol droplet to be a hemisphere in contact with the glass substrate. In that case, the wall friction would be

$$F_W = \int_A \eta \frac{\partial v_x}{\partial y} dA \approx A \eta \frac{v_{\text{drop}}}{h_{\text{drop}}} \quad (4)$$

where  $A = 10.18 \times 10^{-6} \text{ m}^2$  is the projected droplet area,  $\eta = 12.0 \times 10^{-3} \text{ Pa}\cdot\text{s}$  is the viscosity of decanol,  $v_{\text{drop}} = 1.5 \times 10^{-3} \text{ m/s}$  is a characteristic value of the droplet velocity, and  $h_{\text{drop}}$  is the characteristic droplet height, calculated from the droplet area and volume ( $V = 5 \text{ }\mu\text{L}$ ) based on the spherical cap approximation. The resulting force is  $F_W = 0.21 \times 10^{-6} \text{ N}$ , which is larger than the fluid drag force (mainly due to the higher viscosity of decanol compared to water) but still well below the surface tension force. Although simple, this order-of-magnitude calculation supports the hypothesis that in principle the gradient of surface tension has sufficient power to cause the droplet movement. At the same time, it should be kept in mind that other mechanisms such as interaction with the glass substrate can also be involved in the propulsion of the droplet.

#### 4. CONCLUSIONS

A new, relatively simple two-phase system exhibiting artificial chemotaxis has been described. It is based on a decanol droplet in an aqueous solution of sodium decanoate, with sodium chloride as a chemoattractant. The range of concentrations in which the system exhibits chemotaxis has been determined, and the parametric dependence of two important characteristics—the induction time and the migration velocity—on the salt concentration gradient has been systematically investigated. It has been demonstrated that this artificial chemotaxis system bears many qualitative similarities with natural chemotaxis systems, namely (i) the ability to perform chemotaxis

repeatedly when the chemoattractant gradients are recreated, (ii) to perform chemotaxis in topologically complex environments, (iii) to select the chemotaxis direction based on the relative strength of alternative chemoattractant sources, (iv) to rest in a dormant state and later respond to a stimuli-responsive chemoattractant release, and finally (v) to deliver a reactive payload toward the chemoattractant source. To the best of our knowledge, this is the first time that an artificial chemotaxis system exhibiting all of the above-mentioned five features has been described. By measuring the concentration dependence of surface tension, order-of-magnitude estimates of the forces acting on the droplet could be made, supporting a hypothesis that a surface tension gradient can be responsible for chemotaxis in this case.

#### ■ ASSOCIATED CONTENT

##### Supporting Information

Movies 1–5. This material is available free of charge via the Internet at <http://pubs.acs.org>.

#### ■ AUTHOR INFORMATION

##### Corresponding Author

\*E-mail [jitka.cejkova@vscht.cz](mailto:jitka.cejkova@vscht.cz) (J.Č.).

##### Notes

The authors declare no competing financial interest.

#### ■ ACKNOWLEDGMENTS

This work was supported by the European Commission FP7 Future and Emerging Technologies Proactive: 270371 (COBRA), 318671 (MICREAgents), 249032 (MATCHIT), and 611640 (EVOBLISS).

#### ■ REFERENCES

- Lodish, H.; Berk, A.; Zipursky, S. L.; Matsudaira, P.; Baltimore, D.; Darnell, J. *Cell Locomotion*. In *Molecular Cell Biology*, 4th ed.; W.H. Freeman: New York, 2000.
- Eisenbach, M. *Chemotaxis*; Imperial College Press: London, 2004.
- Lackie, J. M. *The Dictionary of Cell & Molecular Biology*; Elsevier Science: Amsterdam, 2012.
- Fournier-Bidoz, S.; Arsenaull, A. C.; Manners, I.; Ozin, G. A. Synthetic self-propelled nanorotors. *Chem. Commun.* **2005**, *4*, 441–443.
- Mano, N.; Heller, A. Bioelectrochemical propulsion. *J. Am. Chem. Soc.* **2005**, *127* (33), 11574–11575.
- Abecassis, B.; Cottin-Bizonne, C.; Ybert, C.; Ajdari, A.; Bocquet, L. Boosting migration of large particles by solute contrasts. *Nat. Mater.* **2008**, *7* (10), 785.
- Agarwal, A.; Hess, H. Biomolecular motors at the intersection of nanotechnology and polymer science. *Prog. Polym. Sci.* **2010**, *35* (1-2), 252–277.
- Upadhyaya, A.; Chabot, J. R.; Andreeva, A.; Samadani, A.; van Oudenaarden, A. Probing polymerization forces by using actin-propelled lipid vesicles. *Proc. Natl. Acad. Sci. U. S. A.* **2003**, *100* (8), 4521–4526.
- Behkam, B.; Sitti, M. Towards hybrid swimming microrobots: Bacteria assisted propulsion of polystyrene beads. *Proc. 28th IEEE (EMBS Annu. Int. Conf.)* **2006**, 2421–2424.
- Nagai, K.; Sumino, Y.; Kitahata, H.; Yoshikawa, K. Mode selection in the spontaneous motion of an alcohol droplet. *Phys. Rev. E* **2005**, *71* (6), 065301.
- Nakata, S.; Matsuo, K. Characteristic self-motion of a camphor boat sensitive to ester vapor. *Langmuir* **2005**, *21* (3), 982–984.
- Sumino, Y.; Kitahata, H.; Yoshikawa, K.; Nagayama, M.; Nomura, S.-i. M.; Magome, N.; Mori, Y. Chemosensitive running droplet. *Phys. Rev. E* **2005**, *72* (4), 041603.

- (13) Lagzi, I.; Soh, S.; Wesson, P. J.; Browne, K. P.; Grzybowski, B. A. Maze solving by chemotactic droplets. *J. Am. Chem. Soc.* **2010**, *132* (4), 1198–1199.
- (14) Hanczyc, M. M.; Toyota, T.; Ikegami, T.; Packard, N.; Sugawara, T. Fatty acid chemistry at the oil-water interface: Self-propelled oil droplets. *J. Am. Chem. Soc.* **2007**, *129* (30), 9386–9391.
- (15) Toyota, T.; Maru, N.; Hanczyc, M. M.; Ikegami, T.; Sugawara, T. Self-propelled oil droplets consuming “fuel” surfactant. *J. Am. Chem. Soc.* **2009**, *131* (14), 5012–5013.
- (16) Ševčíková, H.; Čejková, J.; Krausová, L.; Příbyl, M.; Štěpánek, F.; Marek, M. A new traveling wave phenomenon of *Dictyostelium* in the presence of cAMP. *Phys. D (Amsterdam, Neth.)* **2010**, *239* (11), 879–888.
- (17) Kessin, R. H. *Dictyostelium: Evolution, Cell Biology, and the Development of Multicellularity*; Cambridge University Press: Cambridge, UK, 2001.
- (18) Song, L.; Nadkarni, S. M.; Bödeker, H. U.; Beta, C.; Bae, A.; Franck, C.; Rappel, W.-J.; Loomis, W. F.; Bodenschatz, E. *Dictyostelium discoideum* chemotaxis: Threshold for directed motion. *Eur. J. Cell Biol.* **2006**, *85* (9–10), 981–989.
- (19) Harada, I.; Furukawa, Y.; Tasumi, M.; Shirakawa, H.; Ikeda, S. Spectroscopic studies on doped polyacetylene and  $\beta$ -carotene. *J. Chem. Phys.* **1980**, *73* (10), 4746–4757.
- (20) Nakata, S.; Iguchi, Y.; Ose, S.; Kuboyama, M.; Ishii, T.; Yoshikawa, K. Self-rotation of a camphor scraping on water: New insight into the old problem. *Langmuir* **1997**, *13* (16), 4454–4458.
- (21) Soh, S.; Bishop, K. J. M.; Grzybowski, B. A. Dynamic self-assembly in ensembles of camphor boats. *J. Phys. Chem. B* **2008**, *112* (35), 10848–10853.
- (22) Nakata, S.; Komoto, H.; Hayashi, K.; Menzinger, M. Mercury drop “attacks” an oxidant crystal. *J. Phys. Chem. B* **2000**, *104* (15), 3589–3593.
- (23) Haidara, H.; Vonna, L.; Schultz, J. Surfactant induced Marangoni motion of a droplet into an external liquid medium. *J. Chem. Phys.* **1997**, *107* (2), 630–637.